

Leon PROCHOWSKI
Wojciech WACH
Jerzy JACKOWSKI
Wiesław PIENIAŹEK

EXPERIMENTAL AND MODEL STUDIES ON THE INFLUENCE OF THE RUN FLAT TIRE DAMAGE ON BRAKING DYNAMICS OF THE MULTI-AXIAL SPECIAL PURPOSE VEHICLE

EKSPERYMENTALNE I MODELOWE BADANIA WPŁYWU USZKODZENIA OPON RUN FLAT NA DYNAMIKĘ HAMOWANIA WIELOOSIOWEGO POJAZDU SPECJALNEGO*

Tire damage, that occurs quite often during operation of special purpose vehicles (building, forest, military, agricultural heavy-duty vehicles), affects a vehicle motion also during sudden braking. Motion of a four-axial vehicle has been analysed in order to evaluate the influence of tire damage (cracking, tearing) on its behaviour during sudden braking and based on that to evaluate the possibilities of driver's reactions to motion disorders resulting from that emergency condition. Using the PC-Crash software, a vehicle model was designed allowing for simulation of special-purpose vehicle motion. The vehicle model includes a possibility of occurring of sudden tire damage when in motion. In such situation a model of cooperation of a tire and a surface is of crucial significance. A semi-empirical, non-linear TMeasy tire model was used. Its parameters were obtained on the basis of the results of the tests performed on 14.00R20 tires with run flat inserts. A vehicle model parameterization was based on the results of the vehicle measurements, however the validation was based on the results of experimental road tests of braking with damaged tires. Performed calculations and simulations indicated that when braking is started a process of vehicle deviation and related motion track modification is initialized. The motion track deviation increases as the initial braking speed is increased.

Keywords: tire use, special purpose vehicle operation, active safety, tire damage, run flat tires, driver training.

Uszkodzenie opony, które dość często pojawia się podczas eksploatacji pojazdów specjalnych (budowlane, leśne, militarne, rolnicze), wpływa na ruch pojazdu, również podczas gwałtownego hamowania. Analizie poddano ruch czteroosiowego pojazdu w celu dokonania oceny wpływu uszkodzenia opon (pęknięcie, rozzerwanie) na jego zachowanie się podczas gwałtownego hamowania, a na tej podstawie oceny możliwości reakcji kierowcy na zaburzenia ruchu wynikające z takiego stanu awaryjnego. Korzystając z programu PC-Crash opracowano model pojazdu umożliwiający symulację ruchu pojazdu specjalnego. Model pojazdu uwzględnia możliwość powstania nagłego uszkodzenia opony w czasie jazdy. W takiej sytuacji decydujące znaczenie ma model współpracy opon z nawierzchnią. Zastosowano nieliniowy semi-empiryczny model opony TMeasy, którego parametry uzyskano na podstawie wyników badań opon 14.00R20 z wkładkami run flat. Parametryzacja modelu pojazdu została oparta na wynikach pomiarów pojazdu, natomiast walidacja na wynikach eksperymentalnych badań drogowych hamowania z uszkodzonym ogumieniem. Przeprowadzone obliczenia i symulacje pokazały, że po rozpoczęciu hamowania następuje proces odchylenia pojazdu i związana z tym zmiana toru jazdy. Odchylenie toru jazdy rośnie wraz ze wzrostem prędkości początkowej hamowania.

Słowa kluczowe: eksploatacja opon, eksploatacja pojazdów specjalnych, bezpieczeństwo czynne, uszkodzenia opon, opony run flat, szkolenie kierowców.

1. Introduction

Difficult conditions of special purpose vehicle operation result in high tire damage risk. The nature of damage varies but it always affects the vehicle traction properties and causes increased driver's effort and driving safety threat. A vehicle with damaged tires (if it is still able to continue a drive, even a short-distance one) has increased motion resistance and it is hard to keep an intended track of motion.

The analyses being carried out further on refer to the braking process of a vehicle equipped with run flat tires. The wheels with that type of equipment can be driven for a short distance after tire damage.

The goal of this paper is to analyse the behaviour of a special purpose vehicle after tire damage (cracking, tearing resulting in complete loss of internal pressure) when driving. A process of sudden braking

after tire damage as a basis for evaluation of driver's abilities to react to that type of motion disorders is being considered. The purpose of performed calculations is a detailed evaluation of the influence of location (position) of damaged tires on the behaviour of a vehicle during sudden braking and most of all on a vehicle motion track and a course of variations of parameters that characterize that motion. Braking from the initial speed of 40 and 80 km/h is considered. The essential attention was paid to a process of validation of a multi-axial vehicle with damaged run flat type tires. There are few available papers including that type of a problem [1, 4, 7, 15, 17]. There are papers concerning the influence of a tire pressure on a vehicle driving properties [2, 10], however there are no works that discuss the influence of tire damage on a process of sudden braking of a multi-axial vehicle.

(*) Tekst artykułu w polskiej wersji językowej dostępny w elektronicznym wydaniu kwartalnika na stronie www.ein.org.pl

Identification of the influence of tire damage on the safety of further vehicle motion can be a source of many indications for vehicle structure improvement and for practical driver training.

2. A model of dynamics of the braking process with damaged tires

Using the PC-Crash software [11], a model of a special purpose vehicle and a driver model were built. The vehicle model includes possibility of simulation of sudden tire damage when driving. The driver model allows for reaction to such situation.

The vehicle model includes a rigid body and 8 wheels with independent suspension and it has 14 degrees of freedom:

$$q = [x, y, z, \varphi, \theta, \psi, \Omega_1, \Omega_2, \Omega_3, \Omega_4, \Omega_5, \Omega_6, \Omega_7, \Omega_8]^T, \quad (1)$$

where: x, y, z – the coordinates of the vector r describing the position of the centre of gravity (CG) of the vehicle body C and the origin of local system of coordinates at the same time in the global system $\{O\}$; the local system $\{C\}$ of coordinates is related to a vehicle and fixed to the vehicle's CG,

φ, θ, ψ – quasi-Euler's angles of system orientation $\{C\}$ in relation to the system $\{O\}$, that is:

φ – roll angle (angle of the body rotation around longitudinal axis x' of the system $\{C\}$),

θ – pitch angle (angle of the body rotation around the transverse axis y' of the system $\{C\}$),

ψ – yaw angle, i.e. angle of body rotation around the vertical axis parallel to the axis z' of the system $\{O\}$,

$\Omega_k, k = 1, \dots, 8$ – the k -th wheel rotation angle.

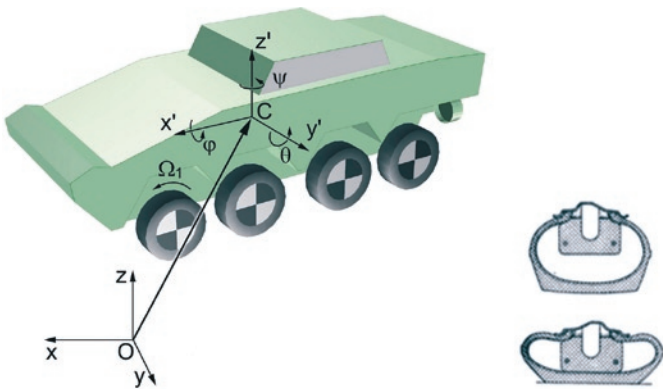


Fig. 1. Vehicle and systems of coordinates, section of a tire with a run flat insert

Vehicle motion equations are expressed with vector dependencies, respectively:

$$m(\dot{\mathbf{v}} + \boldsymbol{\omega} \times \mathbf{v}) = \sum_{i=1}^n \mathbf{F}_i, \quad (2)$$

$$\mathbf{T}\dot{\boldsymbol{\omega}} + \boldsymbol{\omega} \times \mathbf{T}\boldsymbol{\omega} = \sum_{i=1}^n \mathbf{M}_i \quad (3)$$

where: m – vehicle mass,

$\mathbf{v} = \dot{\mathbf{r}}$ – velocity of the CG expressed in the global system $\{O\}$,

$\dot{\mathbf{v}} = \ddot{\mathbf{r}}$ – change of the CG velocity in $\{O\}$,

\mathbf{r} – vector from the origin of the inertial system $\{O\}$ to the vehicle's CG in $\{O\}$,

\mathbf{F}_i and \mathbf{M}_i – respective external forces and moments acting on the vehicle body in $\{C\}$,

\mathbf{T} – tensor of inertia of the vehicle in relation to the centre of mass $\{C\}$,

$\boldsymbol{\omega}$ – angular body velocity vector in $\{C\}$.

Mass deviation moments were neglected so tensor \mathbf{T} looks as follows:

$$\mathbf{T} = \begin{bmatrix} I_{x'} & 0 & 0 \\ 0 & I_{y'} & 0 \\ 0 & 0 & I_{z'} \end{bmatrix}, \quad (4)$$

where: $I_{x'}, I_{y'}, I_{z'}$ – main central moments of inertia of the vehicle.

Interaction between a wheel and a road was described by means of non-linear TMeasy tire model [14, 16]. It allows for determination of forces and moments generated by a tire (affecting the suspension and the vehicle) on the basis of the results of experimental tests. The results of the tests performed on 14.00R20 tires with run flat inserts [12] were used, as the analysed vehicle is equipped with that type of tires. The TMeasy model needs to include on each wheel the longitudinal and lateral force depending on the longitudinal and lateral slip respectively:

$$F_X(s_X, t) = \mu \mu_X(s_X) \cdot F_Z(t) \quad (5)$$

$$F_Y(s_Y, t) = \mu \mu_Y(s_Y) \cdot F_Z(t) \quad (6)$$

where: μ – coefficient of friction;

$F_Z(t)$ – current value of the vertical reaction of the road on the wheel;

Normalized longitudinal and lateral forces depending on longitudinal and lateral slip respectively

$$\mu_X(s_X) = \frac{X_K(s_X)}{Z_K} \quad (7)$$

$$\mu_Y(s_Y) = \frac{Y_K(s_Y)}{Z_K} \quad (8)$$

are determined during the tire tests, while Z_K means vertical reaction during the study. Examples of characteristics $X_K(s_X)$ and $Y_K(s_Y)$ and notation applied are shown in figure 2.

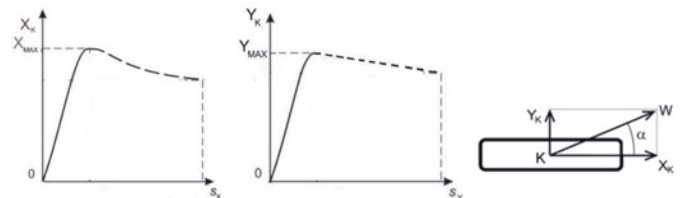


Fig. 2. Tangential reactions of the road on the wheel [13], K – centre of the tire-road contact

Braking force F_H , applied by a driver, is used for calculation of longitudinal force F_X considering the properties of applied tire model. At the same time, the resultant tangential force W (compare fig. 2) cannot exceed the following value:

$$W \leq \mu F_Z(t) \quad (9)$$

During simulation of the vehicle motion, the values, required at each moment of the time, of longitudinal force F_X and lateral force F_Y of the k -th wheel are calculated considering the local coefficient of friction and current reaction of the road on the whe F_Z . It allows for considering variation of traction at the moment of tire damage. In the modelling process it is assumed that damage of a tire with a run flat insert results in:

- decrease of radial tire stiffness;
- change in the cornering stiffness characteristics and most of all decrease of resistance to the side slip;
- rolling resistance increase.

Properties of a tire after damage were modelled by modifications of its characteristic – an example is shown in figures 3 and 4.

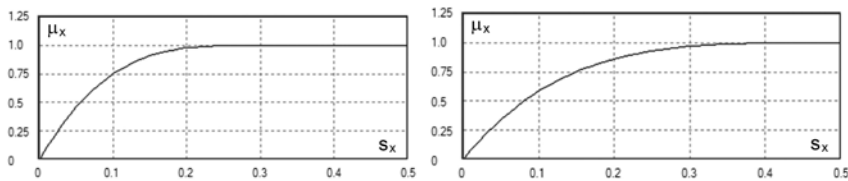


Fig. 3. Normalized longitudinal force as a function of longitudinal slip $\mu_x=f(s_x)$: a) good tire, b) damaged tire

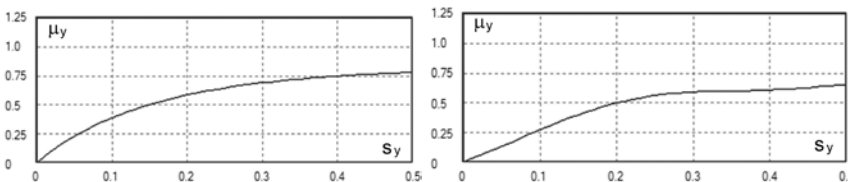


Fig. 3. Normalized lateral force as a function of lateral slip $\mu_y=f(s_y)$: a) good tire, b) damaged tire

3. Determining vehicle model parameters and characteristics

A model of vehicle dynamics and driver's actions was developed by using PC-Crash 9.2 software. It was assumed that the mass is evenly distributed around the axis x' of the vehicle body. The vehicle model has 4 steering wheels turning around vertical axes, going through their centres and parallel to axis z' .

When the suspension deflects the wheels are moving parallel to the vertical vehicle axis z' . Tire characteristics are non-linear. A moment of wheel inertia in relations to the rotation axis was included. The wheels are suspended independently by means of springing and damping elements of characteristics reduced to the wheel centres. The force in the suspension is a sum of the springing and damping forces and it is described by the sectional linear characteristic.

Braking is executed by individual force values of each wheel (in order to simulate the damages) and considering the tire model and a braking force limiter. The characteristic of the braking force limiter has a significant influence on the course of braking. A limiter with characteristic presented in figure 5, was installed on the vehicle model axes 3 and 4. Its influence on the longitudinal rear axles forces values during braking F_{Xt} results from the following dependency:

$$q_t = \frac{F_{Xt}}{Q} \leq q_{t0} \quad (10)$$

where: Q – vehicle weight,
 $z = a_H/g$, a_H – braking deceleration,

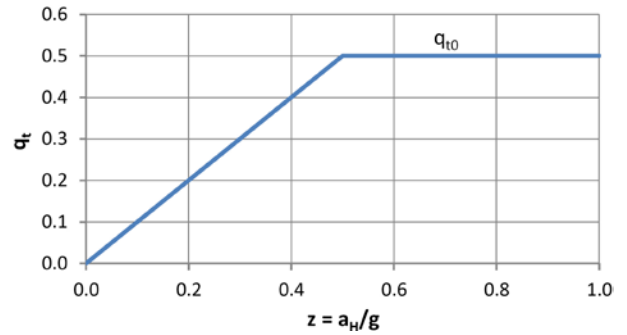


Fig. 5. Braking force limiter characteristics

q_{t0} – characteristic of the braking force limiter according to fig. 5.

The main determination of model parameters and characteristics was made on the basis of vehicle measurements described in [8, 12]. Then the vehicle was used for the braking tests with damaged tires. Some input data was supplemented on the basis of values generated in PC-Crash for that vehicle category. Collected data made an exit point in the model parameterization process. Figure 6 shows adopted vehicle wheel numbering.

The driver model executes a set function of the steering angle of steered wheels as an input affecting the vehicle model. A PID (Proportional- Integral- Derivative) regulator was used for that purpose.

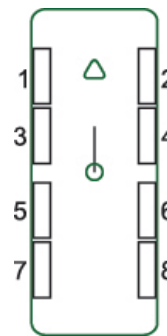


Fig. 6. Wheel numbering

4. Validation process

4.1. Initial calculations and their results

The validation process is an action performed in order to evaluate in what degree a developed calculation software and applied models have properties in accordance with a tested vehicle in the aspect of a course of sudden braking process with damaged tires. A described process leads to obtaining simulation results that successfully reflect behaviour of a tested vehicle including the results of tire damage. Three stages of the validation process were carried out. The first stage includes initial calculations where the process of vehicle braking with good tires was analysed. The second stage includes braking with one damaged tire and in the third stage analysed was the braking with two damaged tires. Corrections of values of some model parameters were made at the next stage in order to decrease the difference between the model response and the object. The tuning of model parameter values was limited to its uncertainty ranges.

The initial calculations analysed the process of braking from the initial speed of 80 km/h. Figure 7 shows time history of three components of the vector of acceleration of the vehicle's CG in the local

system {C}. The effect of the body pitch during braking, resulting in tire and suspension deflection, confirm the values of the vertical body acceleration, presented in figure 7. Typical longitudinal vehicle body vibrations are visible at the moment of stopping the vehicle.

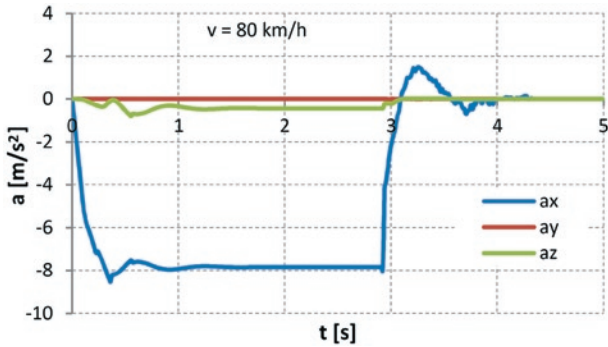


Fig. 7. Time history of three components of vehicle's CG acceleration

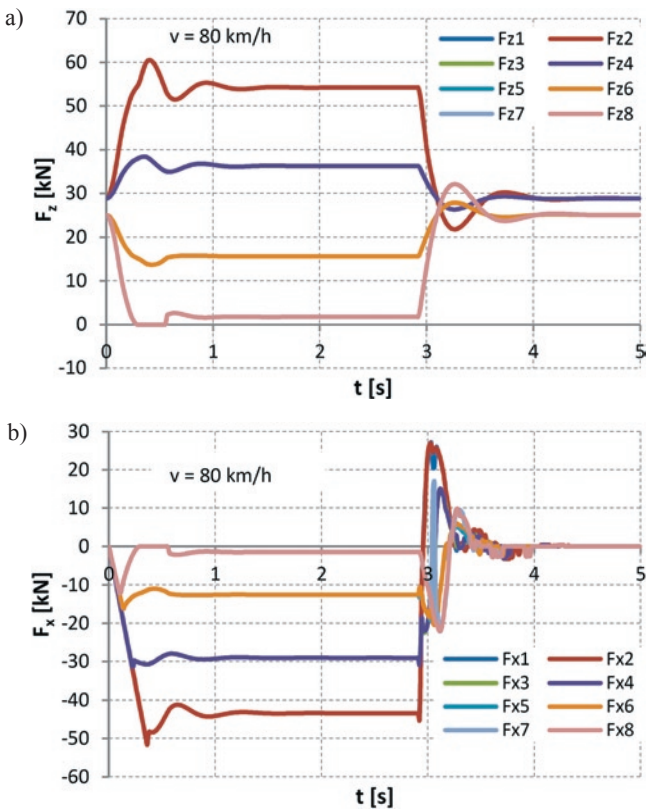


Fig. 8. Time histories of vertical reaction of the road on the tires $F_{z_i}(t)$ (a) and longitudinal tire forces $F_{x_i}(t)$ (b); wheel numbering according to Figure 6

Figure 8 shows a time history of the tire vertical $F_{z_i}(t)$ and longitudinal forces $F_{x_i}(t)$. Because of the symmetry of longitudinal forces on the right side and left side wheels of the vehicle (roadworthy vehicle), time histories of vertical forces of both wheels of each axle are the same, i.e. they overlap. When braking, a significant body pitch occurs and as a result the wheels 7 and 8 lost the contact with the road. Due to that tilt, braking forces of further wheels are more and more lower. The loss of contact between the wheels and the road, shown in fig. 8, results in decrease of the value F_x (fig. 8b) to zero on the wheels 7 and 8.

The results of the roadworthy vehicle braking simulation correctly reflect the properties of the vehicle braking process.

4.2. Model validation on the basis of braking simulation for a vehicle with one damaged tire

The braking tests of a vehicle with damaged tire were carried out in a *fixed control* mode. However, small modifications of the steering wheel angle, which could have been caused by the driver unwillingly at asymmetrical braking, were found in recorded time histories. It was used as a kinematic input in the simulation process, while the measured history of braking deceleration made a basis for braking force generation in the model.

In figures from 9 to 11, a dotted line shows the measurement results obtained during braking from $v = 62$ km/h of the vehicle with a damaged tire no. 2. Accelerations were digitally filtrated by the CFC 100 filter. It is a low-pass Butterworth's filter made according to the SAE J211 standard. The analysed figures also show the results of simulations, marked with a bold continuous line. Bold lines in fig. 9 can be treated as an input affecting the vehicle model.

It was stated that the model properly reacts to the tire damage. Observed differences (vehicle – model) of the pitch angle values $\theta(t)$ can result from the variability of wheel suspension characteristics (hydropneumatic suspension) and presence of dry friction. Obtained results of simulation calculations properly reflect the measurements that were obtained during the vehicle tests. Results of transverse displacement of the vehicle's CG during braking ($y(t)$ in fig. 11) are the significant factor of the quality evaluation for assumed tire model. After driving for over 40 m on the road and in the presence of various wheel steer angles, the difference between the values of transverse displacement of the model and the vehicle is lower than 0.2 m.

4.3. Model validation on the basis of braking of the vehicle with two damaged wheels (wheels no. 2 and 4)

At this stage of calculations the measurement results obtained during vehicle braking with two damaged tires were used. They are compared with respective model calculation results in figures 12–14.

During braking test from 61 km/h a modification of the steering wheel angle by over 18° was observed, which is related to the previously described reasons. So the responses of the vehicle model to the same input (presented in fig. 12) are compared in figures 13 and 14 with responses of the real object.

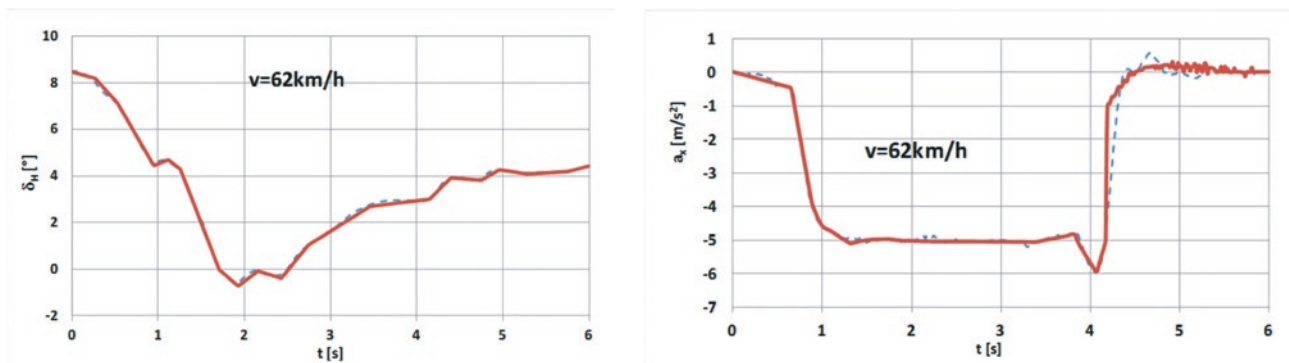


Fig. 9. Steering wheel rotation angle $\delta_H = f(t)$ and longitudinal acceleration $a_x(t)$; dotted line – vehicle, bold line – model

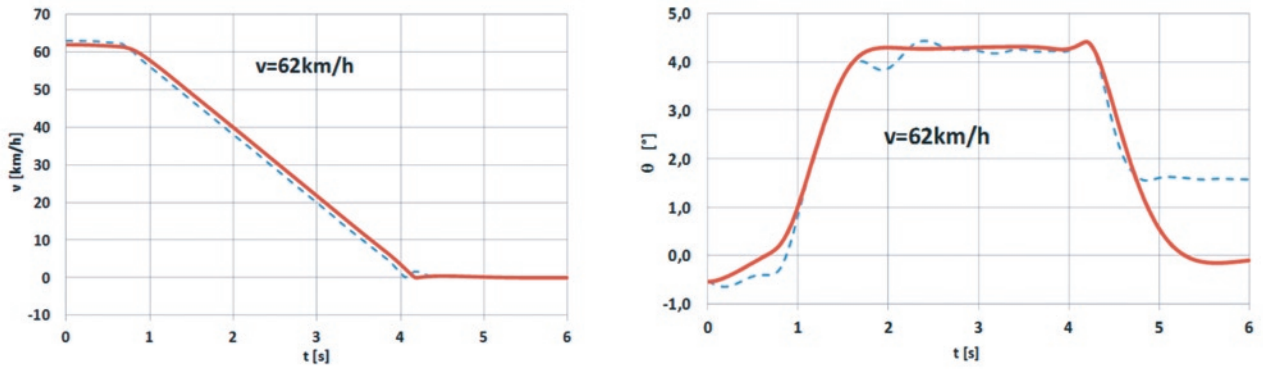


Fig. 10. Velocity of the vehicle's CG $v(t)$ and the body pitch angle $\theta(t)$; line description as under figure 9

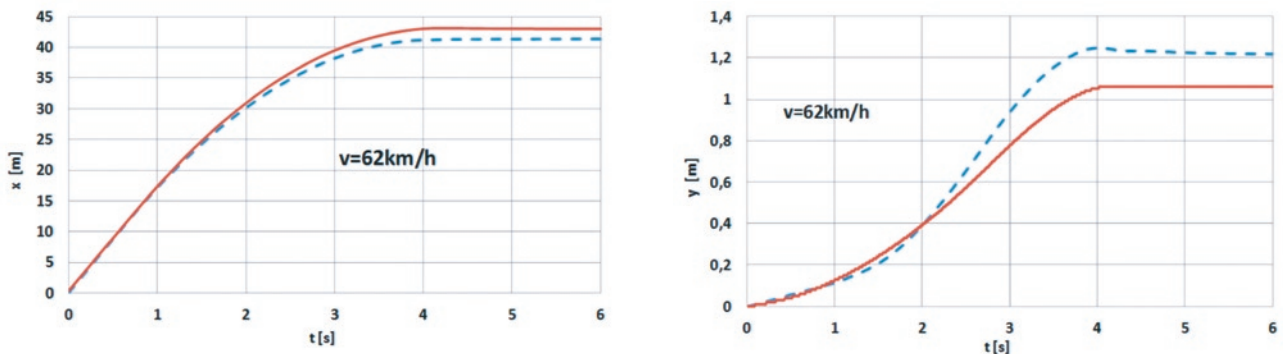


Fig. 11. Longitudinal $x(t)$ and lateral $y(t)$ displacement of the CG (braking path); line description as under fig. 9

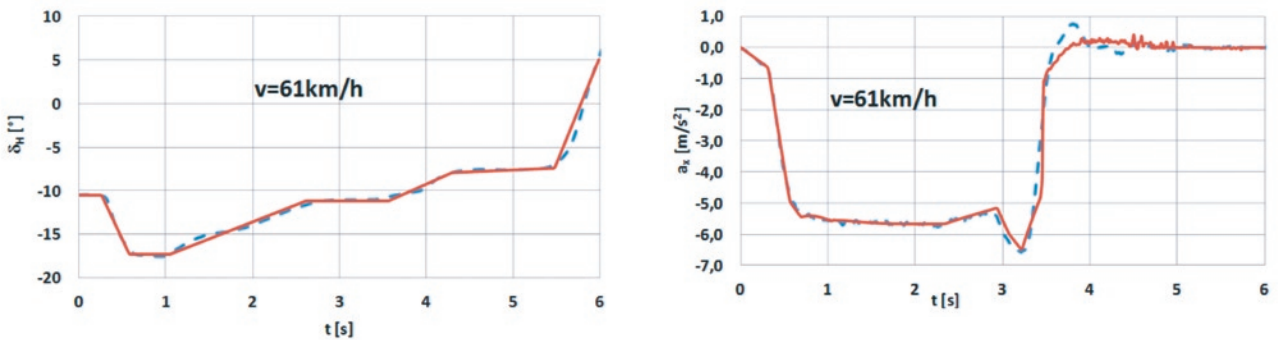


Fig. 12. Steering wheel angle $\delta_H(t)$ and longitudinal acceleration $a_x(t)$; dotted line – vehicle, bold line – model

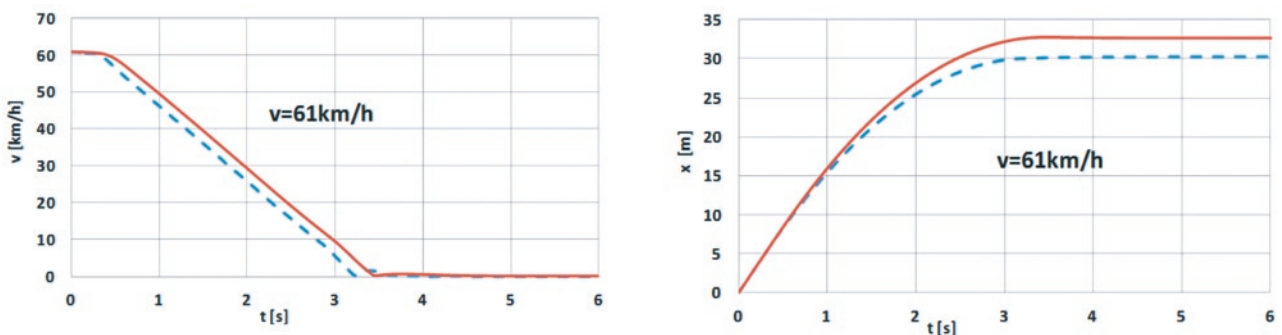


Fig. 13. Velocity of the vehicle's CG $v(t)$ and longitudinal displacement $x(t)$; line description as under fig. 12

Previously described effects (unintended driver's reactions) and effects caused by damaged tires result in low values of yaw rate (below 0.05 rad/s, compare fig. 14) and lateral acceleration, which does not exceed 0.6 m/s². Obviously at such low lateral interactions, the

presence of freeplay and friction in the steering system and suspension have a significant influence on the vehicle trajectory. Despite the model does not include these factors, its reaction to the defined inputs is very similar to the real behaviour of the vehicle with dam-

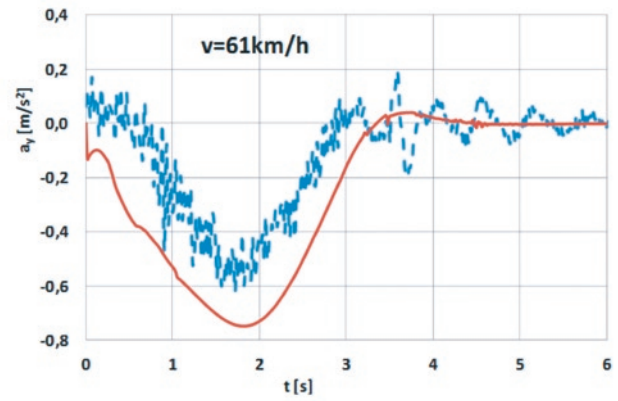
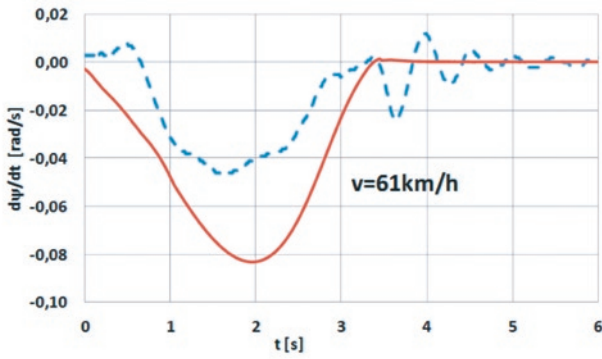


Fig. 14. Yaw rate of the vehicle $\dot{\psi}(t)$ and lateral acceleration; line description as under fig. 12

aged tires. In both simulations (p. 4.2 and 4.3) a low deviation of the vehicle trajectory from the rectilinear track was found, which results not only from the presence of damaged tires but also from the action of the driver who made a correcting turn of the steering wheel. Values of lateral displacement of the vehicle's CG notably depend on a time history of the steering wheel angle.

In the applied results of both braking tests, the time history of that angle was definitely different. Due to a fast tire destroying and wear process, the braking tests with damaged tires were not repeated (high tire cost).

Validation calculations confirm a proper model reaction to tire damage and vehicle braking. So it can be assumed that the model properly reflects the vehicle properties in the area significant for the purpose of this paper.

5. Essential calculations

5.1. Preparation of calculations

16 braking tests were prepared for the execution of the calculation goal, where the location of the wheels with damaged tires was changed. Braking in the first seven tests was started from the speed of 40 km/h, and in the following seven ones it was started from 80 km/h. In the next two test calculations (T0/40 and T0/80) a simulation of the model braking with roadworthy tires was carried out. Arrangement of wheels with damaged tires is shown in figure 15.

Selection of speed values for test calculations was based on the following reasons:

- at $v \cong 60$ km/h braking process disruptions are small (compare the vehicle test results in p. 4.2 and 4.3);
- maximum speed with damaged tires should not exceed 80km/h.

Considering the initial calculation results and the above reasons, the following plan of the test calculation execution has been prepared:

1. The initial drive at constant speed of 40 or 80 km/h for 0.5 s. Tires are fully operational at that stage of the test. The driving torque on the wheels balances the motion resistance.

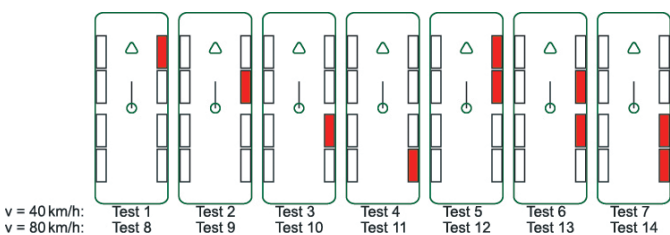


Fig. 15. Arrangement of wheels with damaged tires (darken wheels) and designation of individual tests

2. There is a sudden damage of tire(s) in 0.5 s and for a short period of time surprised driver is preparing a reaction, and at the same time the model motion parameters are stabilized, and rolling resistance of a damaged wheel(s) increases from $f_f=0.01$ to 0.05. On the basis of [6, 9] it was assumed that the length of time when a driver works out a reaction to analysed incident related to tire damage amounts to 1.5 s.
3. After $t = 0.5 + 1.5 = 2.0$ s the driver models begins sudden braking that would last until the vehicle is stopped. Deceleration increases linearly for $t_n = 0.4$ s, until reaching a value of $a_x=5-6$ m/s². All wheels were not blocked in order to avoid vehicle drifting but trends resulting from the operation of damaged wheels appeared.
4. The example of the time history of braking is shown in figure 16.

All calculation tests were conducted out at fixed steering wheel (fixed control). It made the result analysis easier in the aspect of the influence of damaged tires on the motion trajectory.

5.2. Results of calculations for braking with one damaged wheel no. 2 or 4, 6, 8

Figures 16 and 17 show time histories of the CG acceleration and vehicle body pitch angle during rectilinear braking from the speed of 40 km/h and 80 km/h with all roadworthy tires (T0/40 and T0/80).

Time histories in these figures are in accordance with a generally known histories of braking process of a roadworthy vehicle. While the majority of values analysed further on has zero values (side slip angle, yaw angle, yaw rate) and therefore they are not shown in figures 16 – 17.

Results of simulations of the braking process of the vehicle with one damaged tire is shown in table 1. In the consecutive tests T1-T4 and T8-T11 practically the same time history of longitudinal acceleration $a_x = a_H = f(t)$ was obtained as during braking of the model with roadworthy tires (fig. 16). Therefore these figures are not included in Table 1.

Due to a presence of a damaged tire (compare calculation plan, $t > 0.5$ s) the CG trajectory deflection from the rectilinear one occurs already when driving without braking. Table 1 shows the increase of side slip angle α_{CG} and body yaw angle ψ at constant yaw rate 0.1–0.2 °/s in time $t = 0.5-2.0$ s. After the beginning of braking, the process of body yawing and related change of the motion trajectory (deflection to the right side, towards the position of a damaged tire) becomes intensified.

During braking from the speed of 40 km/h observed motion trajectory deflection from the straight track (transverse displacement $y(t)$ and yaw angle $\psi(t)$) are low (compare table 1 and 3). A driver can correct the track of motion without any problem, irrespectively of a location of a damaged wheel. The situation is different when braking

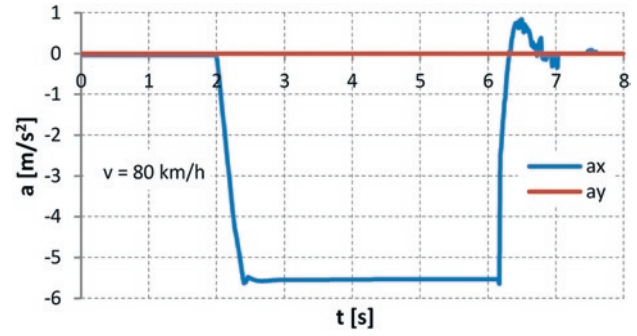
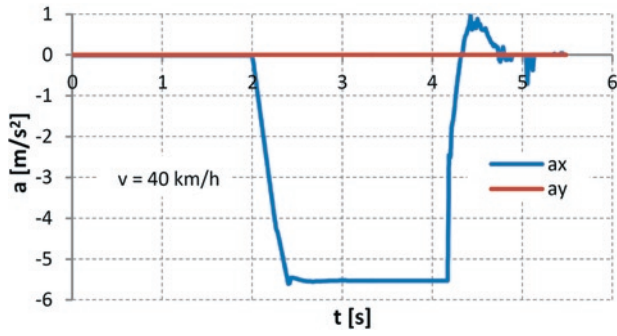


Fig. 16. Components of CG acceleration $a_x(t)$ and $a_y(t)$ in the local system $\{C\}$: a) $v = 40$ km/h, b) $v = 80$ km/h

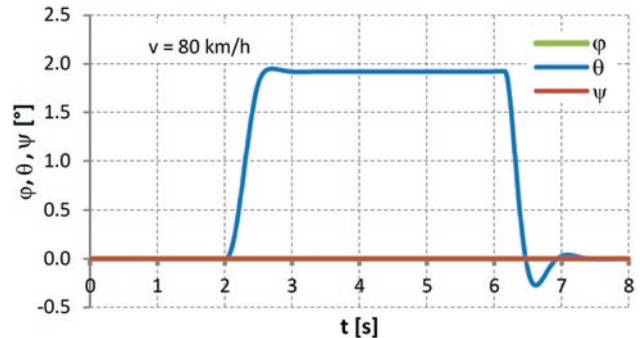
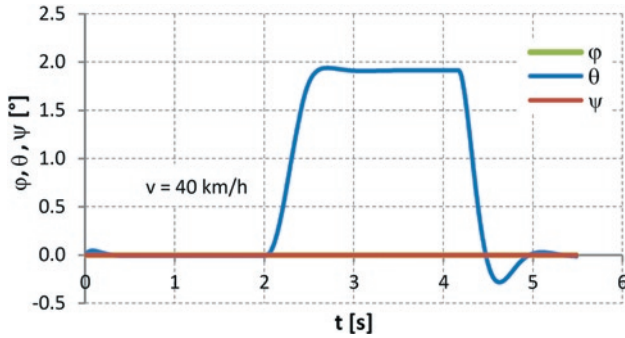


Fig. 17. Roll ϕ , pitch θ and yaw ψ ; a) $v = 40$ km/h, b) $v = 80$ km/h

from the speed of 80 km/h. Values of deflection from the straight line of motion in fact depend on the location of a damaged wheel and resultant wheel load. The lowest deflection occurs in case of damaged wheel no. 6, and the highest in case of a damaged wheel no. 8. Then $\psi(t)$ it reaches 17.6° at the end of braking T11, and the extreme value of the yaw rate amounts to about $10^\circ/\text{s}$ (Table 4). These are significant values and clearly visible. Presence of one underinflated tire has a small influence on the braking distance compared to the roadworthy vehicle braking (table 3 and 4).

5.3. Results of braking calculations for two damaged wheels no. 2-4, 4-6, 6-8

Table 2 shows results of simulation calculations of the braking process of the model with two damaged wheels located in three different places at the right side of the vehicle. The values, previously presented in table 1, were compared.

A time history of longitudinal acceleration $a_x(t)$ was added, because during braking from $v = 80$ km/h significantly differs from the one presented in figure 16b. These differences result from high values of the vehicle yaw angle and tire lateral slip drifting that caused transverse position of the vehicle (compare fig. 18) and thereby reduction of its longitudinal displacement.

Tables 3 and 4 compare the values of longitudinal displacement $x(t)$ of the vehicle's CG in individual tests, from the moment of stepping on the brake pedal until stopping the vehicle. The specification also includes results of calculations for the roadworthy vehicle. Presence of damaged tires has a small influence on the braking distance at the speed of 40 km/h. While the influence of two damaged tires on a braking time history at the speed of 80 km/h is high and results in a significant vehicle yaw from a rectilinear motion track. Reduction of longitudinal displacement $x(t)$ in the tests no. T12-T14 compared to T8-T11 results from drifting of the rear part of the vehicle at the final stage of motion and thereby the use of the lateral components of the tire reaction which was higher than the longitudinal components in that situation.

Values of the vehicle yaw angle during braking at $v = 40$ km/h are low, while at braking from $v = 80$ km/h (the vehicle with two damaged wheels) the vehicle rotates and drifts. So taking into account that braking variant, the most dangerous location of damaged wheels is respectively: 6 and 8 (test 14), 4 and 6 (test 13) as well as 2 and 4 (test 12).

Yaw rates in the braking tests from the speed of 40 km/h (T5 to T7) do not exceed 0.02 rad/s, while at the speed of 80 km/h (T11, 12 and 13) they are significant and almost 70 times higher than at the speed of 40 km/h. Yaw rate increase results in high lateral acceleration values. During braking at the speed of 40 km/h they do not exceed 0.13 m/s^2 , while at the speed of 80 km/h lateral acceleration exceeds 7 m/s^2 (table 4), i.e. it reaches the values that often result in the vehicle rollover. It results from decrease in wheel loads of the axle 3 and 4 during braking and therefore also from the reduced potential of high lateral reactions on these axes. Moreover, a potential of lateral reactions decreases when damaged tires appear (compare fig. 4).

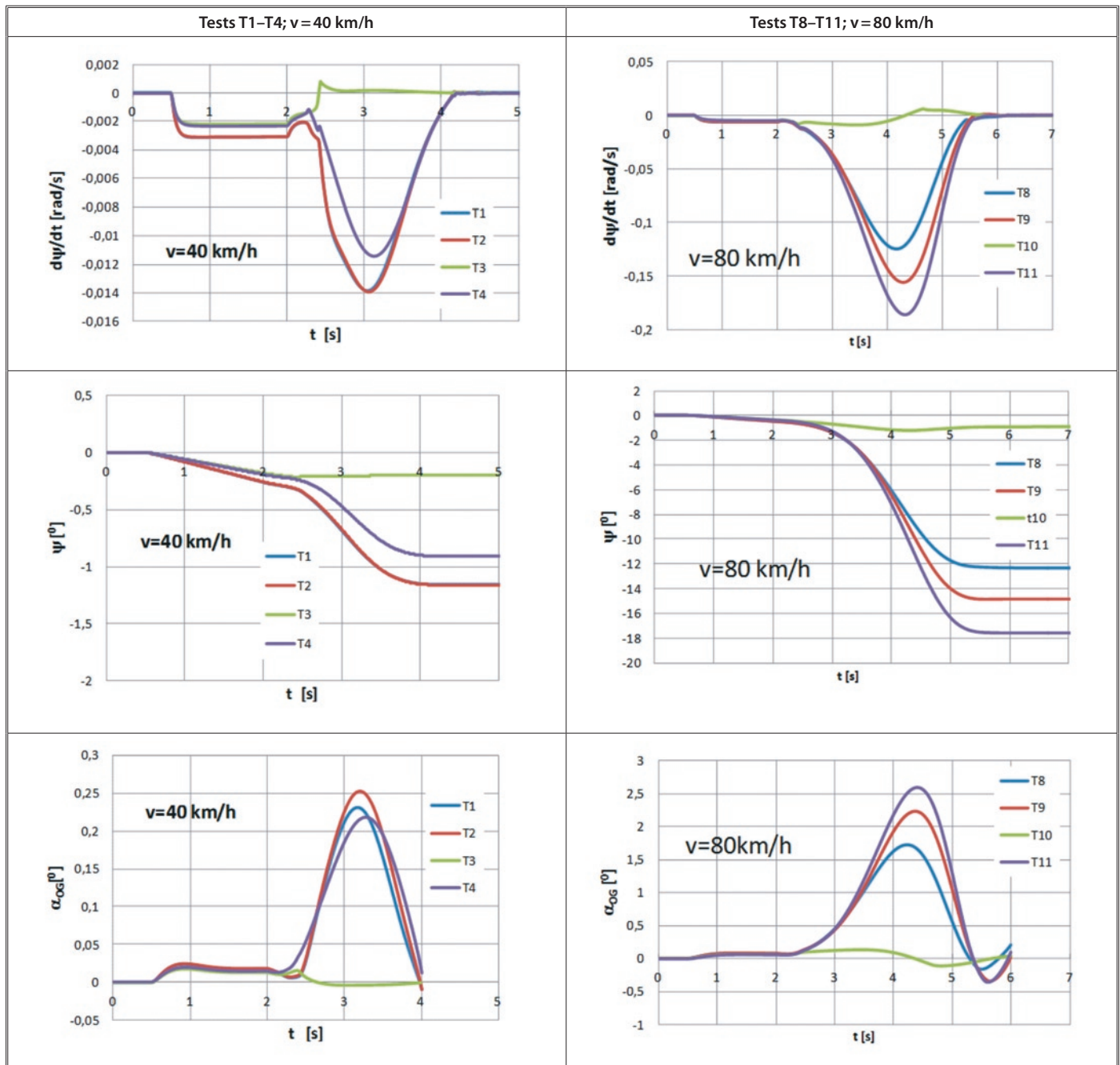
In the braking tests at the speed of $v = 80$ km/h with two damaged wheels, i.e. T12-14 there is a temporary loss of contact between the wheels 6 and 8 and the road during drifting of the rear part of the vehicle as indicated calculations of wheel vertical forces.

6. Summary and conclusions

Built models, performed process of their validation and obtained results of simulations, allowed for identification of the influence of damaged tires and their location in a vehicle on the safety of the sudden braking process of a special purpose vehicle with *run flat* tires. Calculations for 16 braking tests were carried out, changing the location of the wheels with damaged tires. The analysis of calculation results in the aspect of evaluation of a driver's reaction abilities allows for making the following statements:

- tire damage affects the movement of a special purpose vehicle;
- after damage of one tire a vehicle still has an ability to brake effectively and its trajectory can be corrected by a driver;
- damage of one wheel practically does not affect the braking distance;

Table 1. The results of braking calculations for a vehicle with one damaged wheel from the speed of 40 km/h (tests T1- T4) and from the speed of 80km/h (tests T8- T11): $d\psi/dt$ – yaw rate, ψ – yaw angle, α_{CG} – side slip angle of the CG



- braking with one damaged wheel from the speed of 40 km/h does not create a serious danger, but this danger gets higher as the initial braking speed increases and the vehicle yaw from a set track of motion towards a damaged tire increases;
- during braking with one damaged wheel, the strongest influence on the vehicle motion occurs in the tests T8 and T9, that is when wheels 2 or 4 are damaged (steered wheels on the right side of the vehicle);
- damage of two wheels significantly affects the vehicle braking process; observed reduction of the braking distance at high driving speed (tests T12 – T14) is related with dangerous drifting of the rear part of the vehicle;
- a significant factor of the movement safety threat includes a vehicle yaw from the set track of motion; this yaw angle does not exceed 2° (test T5) with two damaged wheels and low driv-

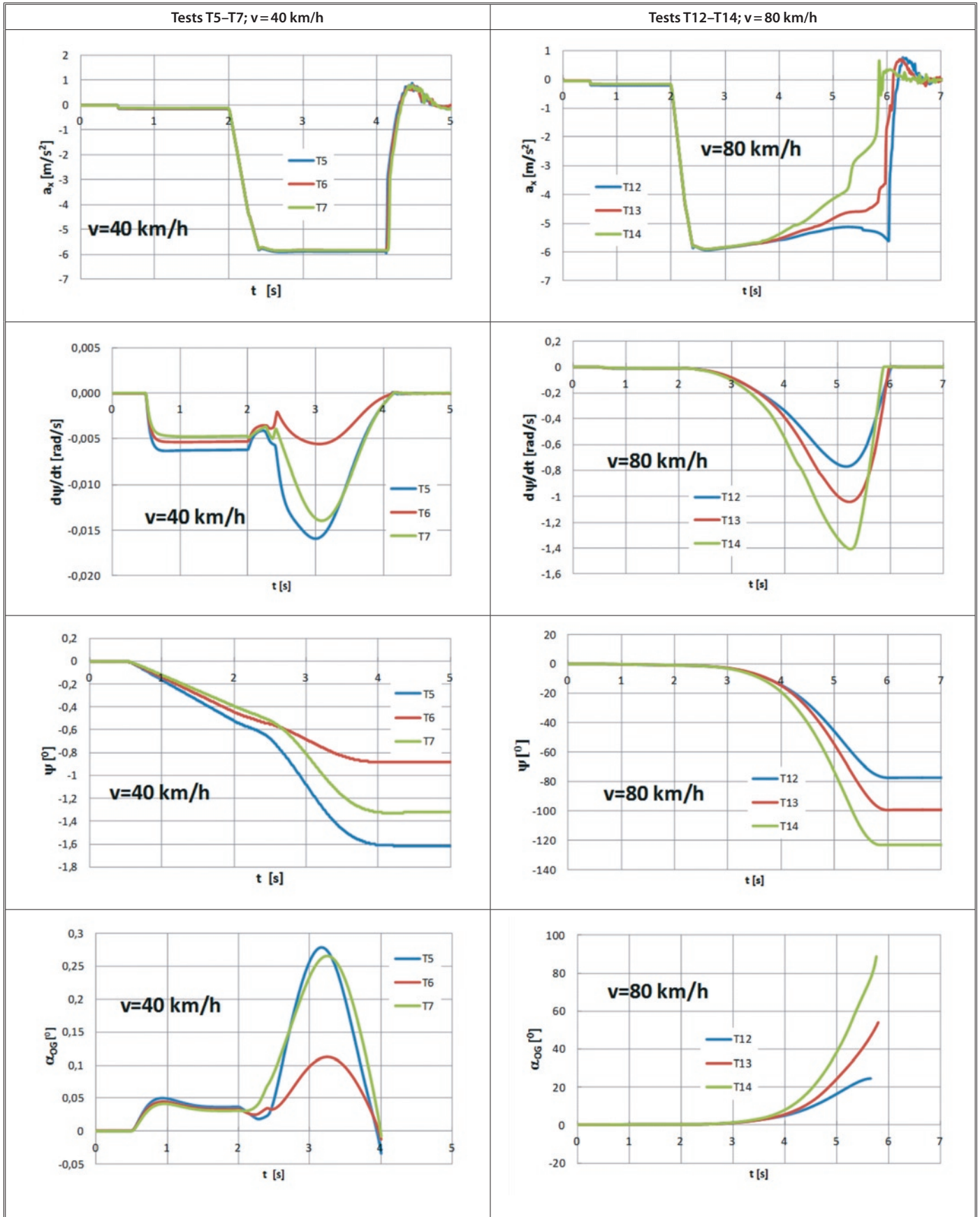
ing speed, but it increases rapidly as the initial braking speed increases and at $v = 80$ km/h the yaw angle exceeds 90° (test T13 and T14), and yaw rate amounts to $100^\circ/s$;

- when braking with two damaged wheels and $v = 80$ km/h there are high lateral acceleration values $5.0\text{--}7.7$ m/s²; these are values that can result in vehicle rollover.

When braking from the speed of 40 km/h, a properly trained driver can correct the motion trajectory, irrespective of the location of a damaged wheel. Extreme yaw rate values at $v = 40$ km/h occur in 1.1–1.2 s from the beginning of braking with one and two damaged wheels.

The tests indicate [3, 5] that a driver can identify and feel horizontal accelerations exceeding 0.02 m/s² and yaw rate of over 0.001 rad/s. So already when a vehicle with one damaged wheel brakes from $v = 40$ km/h, the physical interactions on a driver (compare table 3) amounts to the values that can “signal” him undergoing changes of the

Table 2. The results of braking calculations for a vehicle with two damaged wheels from the speed of 40 km/h (tests T5- T7) and from the speed of 80km/h (tests T12- T14): a_x – longitudinal acceleration, $d\psi/dt$ – yaw rate, ψ – yaw angle, α_{CG} – side slip angle of the CG



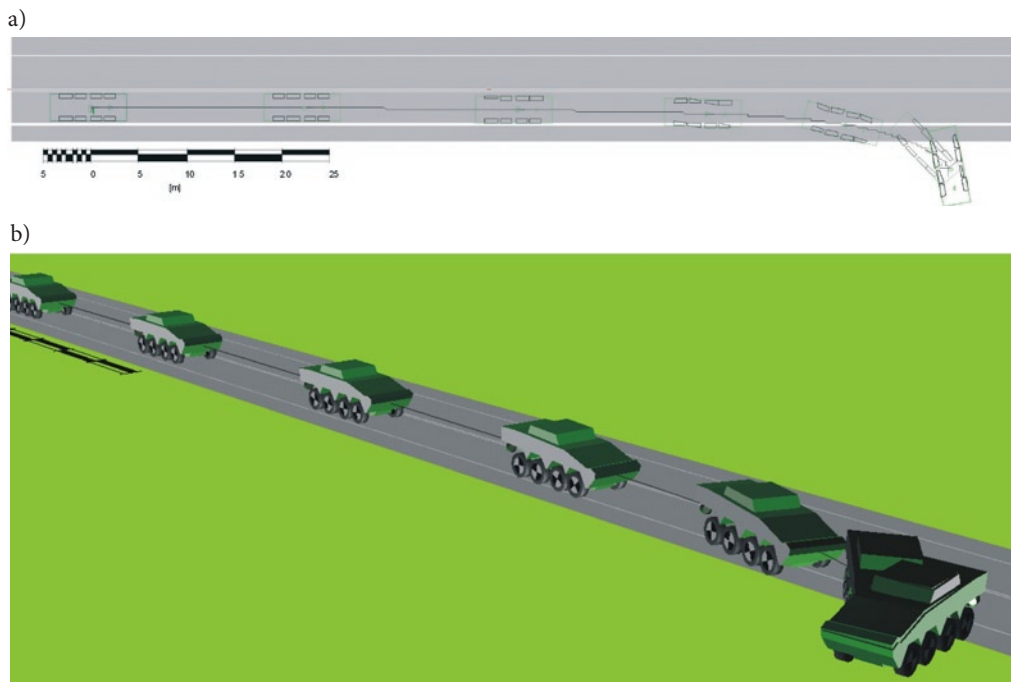


Fig. 18. Road lane and consecutive vehicle positions at 1.0 s time interval, test T12; a) plan view, b) spatial view

Table 3. Extreme values (WE) and final values (WK) of the vehicle body motion parameters depending on a location of damaged tires; braking from $v = 40\text{km/h}$

Specification	T0/40	T1	T2	T3	T4	T5	T6	T7
Longitudinal displacement of the vehicle's CG, [m]	12.85	12.71	12.71	12.85	12.87	12.45	12.58	12.68
Transverse acceleration, WE; $[\text{m/s}^2]$	0	0.06	0.06	0.01	0.10	0.10	0.04	0.13
Yaw rate, WE; $[\text{rad/s}]$	0	-0.014	-0.014	-0.002	-0.01	-0.02	-0.005	-0.01
Yaw, WK; $[\circ]$	0	-1.16	-1.16	-0.21	-0.91	-1.62	-0.88	-1.32
Side slip, WE; $[\circ]$	0	0.02	0.03	0.01	0.22	0.28	0.11	0.27
Lateral displacement, WK; [m]	0	-0.10	-0.09	-0.05	-0.07	-0.16	-0.12	-0.13

Table 4. Extreme values (WE) and final values (WK) of the vehicle body motion parameters depending on a location of damaged tires; braking from $v = 80\text{km/h}$

Specification	T0/80	T8	T9	T10	T11	T12	T13	T14
Longitudinal displacement of the vehicles' CG. [m]	47.58	47.43	47.34	47.49	47.61	45.63	45.50	44.95
Transverse acceleration, WE; $[\text{m/s}^2]$	0	1.8	2.0	0.3	2.4	5.2	6.3	7.7
Yaw rate, WE; $[\text{rad/s}]$	0	-0.12	-0.15	-0.01	-0.18	-0.77	-1.04	-1.41
Yaw, WK; $[\circ]$	0	-12.3	-14.9	-1.23	-17.6	-77.6	-98.9	-123.3
Side slip, WE; $[\circ]$	0	1.71	2.24	0.13	2.54	24.2	53.7	88.9
Lateral displacement, WK; [m]	0	-2.71	-2.96	-0.62	-3.33	-6.15	-5.99	-6.32

motion trajectory. It is important as in critical situations a driver reacts not only to observed motion track deflection from a set track but also to perceived physical signals.

The situation is different in case of braking at the speed of 80 km/h with two damaged tires. Then the vehicle yaw rate amounts to $100^\circ/\text{s}$, and lateral acceleration even to 7 m/s^2 . At the speed of $v = 80 \text{ km/h}$ the extreme values of yaw rate occur in 2.2–2.3 s from the beginning of braking with one damaged tire and in 3.2–3.3 s in a vehicle with two damaged wheels. The wheels on one side of the vehicle detach from the road. So the critical situation in the vehicle behaviour occurs.

The results of the tests and analyses indicate that driver's operation after sudden tire damage is of crucial significance to the vehicle motion

safety [1, 17]. Practical driver training within that scope is expensive and dangerous. Therefore there is a need to obtain knowledge on the basis of reliable models of simulation of vehicle motion during braking. The results of this article can be also used in the process of programming of driving simulators for training the special purpose vehicle drivers. A key role of tire inserts, that allowed for a limited time vehicle motion in analysed situations, deserves a separate emphasis.

A part of this paper was prepared according to the Project OR 00008312, financed by the Ministry of Science and Higher Education.

References:

1. Blythe W., Day T. D., Grimes W. D., 3-Dimensional Simulation of Vehicle Response to Tire Blow-outs, SAE Technical Paper 980221; Warrendale PA 1998.
2. Ejsmont J., Jackowski J., Luty W., Motrycz G., Stryjek P., Świeczko-Żurek B., Analysis of rolling resistance of tires with Run Flat insert, *Key Engineering Materials* 2014; 597: 165-170.
3. Fard M., A., Ishihara T., Inooka H., Dynamics of the head-neck complex in response to the trunk horizontal vibration: modeling and identification, *Journal of Biomechanical Engineering* 2003; 125(4): 533-539.
4. Grover C., Lambourn R. F., Smith T. L., Walter L., Braking and manoeuvring characteristics of incorrectly inflated low-profile and run-flat tyres, [in:] *Proceedings of the 16th Annual Congress of the European Association for Accident Research and Analysis (EVU)*, Institute of Forensic Research Publishers, Kraków 2007; 181-213.
5. Jex H., R., Roll Tracking Effects of G-vector Tilt and Various Types of Motion Washout, *Proceedings of 14 Annual Conference on Manual Control*, University of Southern California 1978.
6. Jurecki R., S., Stańczyk T., L., Jaśkiewicz M., J., Driver's reaction time in a simulated, complex road incident, *Transport*, 2014 <http://dx.doi.org/10.3846/16484142.2014.913535>.
7. Lozia Z., Simulation Tests of Biaxial Vehicle Motion after a Tire Blow-out, SAE Technical Paper 2005-01-0410; Warrendale PA 2005.
8. Lozia Z., Guzek M., Pieniążek W., Zdanowicz P., Methodology and examples of results of simulation tests on a motion of a multi-axial special vehicle in explosive tire damage conditions, *Zeszyty Naukowe Instytutu Pojazdów – Proceedings of the Institute of Vehicles* 2012; 4(90): 19-42.
9. Olson P. L., Forensic aspects of driver perception and response, Lawyers & Judge Publishing Co, Tuscon 1996.
10. Parczewski K., Effect of tyre inflation pressure on the vehicle dynamics during braking manoeuvre. *Eksploatacja i Niezawodność – Maintenance and Reliability* 2013; 15(2): 134-139.
11. PC-Crash, A simulation program for vehicle accidents. Operating and technical manual, Version 10.0, Dr. Steffan Datentechnik, Linz, Austria 2010.
12. Collective paper, Experimental and simulation tests on multi-axial vehicle dynamics in tire damage conditions, Publishing of the Cracow University of Technology, Cracow 2012.
13. Prochowski L., Motor Vehicles. Mechanics of Movement, WKŁ, 2nd Edition, Warsaw 2009.
14. Rill G., Simulation von Kraftfahrzeugen, Vieweg & Sohn Verlag GmbH, Braunschweig/Wiesbaden 1994.
15. Robinette R., Deering D., Fay R. J., Drag and Steering Effects of Under Inflated and Deflated Tires, SAE Technical Paper 970954; Warrendale PA 1997.
16. Wach W. Simulation of vehicle accidents using PC-Crash, Institute of Forensic Research Publishers, Cracow 2011.
17. Zębala J., Wach W., Ciępka P., Janczur R., Bypassing manoeuvre driving a car with reduced and no tire pressure, [in:] *Proceedings of the 22th Annual Congress of the European Association for Accident Research and Analysis (EVU)*, Published by EVU, Firenze 2013, 145–155.

Leon PROCHOWSKI

Faculty of Mechanical Engineering
Military University of Technology
ul. Gen. Sylwestra Kaliskiego 2, 00-908 Warsaw, Poland

Wojciech WACH

Institute of Forensic Research
ul. Westerplatte 9, 31-033 Cracow, Poland

Jerzy JACKOWSKI

Faculty of Mechanical Engineering
Military University of Technology
ul. Gen. Sylwestra Kaliskiego 2, 00-908 Warsaw, Poland

Wiesław PIENIĄŻEK

Faculty of Mechanical Engineering
Cracow University of Technology
al. Jana Pawła II 37, 31-864 Cracow, Poland

E-mails: lprochowski@wat.edu.pl, wwach@ies.krakow.pl,
jjackowski@wat.edu.pl, wupe44@gmail.com
